Robust vibration-activated lubricity

Arnab Bhattacharjee
University of Delaware
Nikolay Garabedian
Karlsruhe Institute of Technology: Karlsruher Institut fur Technologie
Brian Borovsky
Saint Olaf College
David Lawrence Burris (dlburris@udel.edu)
University of Delaware https://orcid.org/0000-0003-2687-7540

Research Article

Keywords: Vibration, QCM, Friction Suppression, Superlubricity, Thermolubricity

Posted Date: July 9th, 2021

DOI: https://doi.org/10.21203/rs.3.rs-675856/v1

Abstract

Friction can be reduced or eliminated when the contact interface is subjected to an external vibration; we refer to this phenomenon here as vibration-activated lubricity. According to prior literature, vibration-activated lubricity is limited to oscillation amplitudes and frequencies that depend strongly on case-specific experimental variables such as the instrument resonance frequency, sliding speed, and slip length of the tribo-pair. This paper aims to overcome these limitations and clarify their origins. Specifically, we used a quartz crystal microbalance (QCM) to directly oscillate the sample at a fixed frequency and at oscillation speeds that exceeded the sliding speed by orders of magnitude. Under these direct oscillation conditions, vibration-activated lubricity persisted for alumina probes ranging from 50-1500 μm in diameter, loads from 20 μN – 5 mN, speeds from 5 μm/s – 1 mm/s, gold and single crystal molybdenum disulfide samples, and two instruments – a custom microtribometer and a commercial atomic force microscope. Under all conditions, vibration-activated lubricity was characterized by very small but non-vanishing friction coefficients (~ 0.01–0.05). Our findings suggest that the following criteria satisfy the conditions for robust vibration-activated lubricity: (1) direct coupling between the oscillator and the sample; (2) probe inertial or spring forces > > available friction; (3) oscillation speed > > sliding speed; (4) oscillation amplitude ≅ or > the slip length.

1.0 Introduction

Friction is known to decrease, sometimes by an order of magnitude or more, when the contact interface is subjected to an external vibration of appropriate direction, frequency, and amplitude [1, 2, 11–20, 3–10] in this paper, we refer to this as vibration-activated lubricity. This phenomenon can have important practical applications including gravity fed particle conveyors [21], the mitigation of stiction and wear in micro and nanoscale devices [22–25], and improved energy efficiency of machines [26]. More importantly, it has important scientific implications due to its potential to select or suppress one or more friction mechanisms. Once understood more completely, vibration-induced lubricity may help answer long-standing questions about the physics of friction and how different mechanisms contribute to friction across length scales.

It is well-known that external vibrations can virtually eliminate friction if they are sufficiently strong to separate surfaces in the normal direction and if the vibrational frequency exceeds the characteristic slip frequency of the friction system (e.g. sliding speed divided by the characteristic slip length) [23, 27–29]. In other words, surfaces are separated before significant lateral forces have the opportunity to develop. However, this ‘hopping’ mode of friction reduction fails to explain the most interesting cases of vibration-induced lubricity. In experiments with boundary lubricated mica, *in-situ* interferometry measurements within the surface forces apparatus (SFA) demonstrated vibration-activated lubricity with a mean interfacial dilatation of no more than 1 angstrom [23]. Thus, they were able to reject the hypothesis that surface separation caused vibration-activated lubricity in their case. Interestingly, the vibration-activated lubricity effect vanished at oscillation frequencies far beyond the resonant frequency of the loading spring (930 Hz) due to poor mechanical coupling. Jeon *et al.* made similar observations using the atomic

force microscope (AFM) [30]. In this case, a lubricant monolayer was applied to gold and friction was minimized when the normal oscillation frequency was about half the resonant frequency (20 kHz) of the instrument; in this case too, the effect vanished as the oscillation frequency increased to well beyond the resonant frequency.

While Heuberger *et al*. showed evidence that molecular relaxations of the lubricant film were responsible for vibration-activated lubricity in their experiments [23], the effect can be just as strong in clean contacts between ideal solids. Experiments by Socoliuc *et al.* showed similar vibration-activated lubricity effects in studies of sharp Si AFM tips against cleaved NaCl and KBr in UHV [31]. Here too, friction was minimized (< 10 pN) when they used a normal oscillation frequency equal to half the normal resonant frequency of the system. At other frequencies, including those matching the torsional resonant frequency of the instrument, they observed large friction forces between 600–900 pN. These effects are not limited to normal oscillations, as shown in otherwise similar studies by Riedo *et al*. [8] At a sliding speed of 8 μm/s, the friction force decreased from 3 AU to 0.5 AU when they subjected the systems to lateral oscillation frequencies near half the normal resonance frequency of the instrument (19.5 kHz); these friction forces increased again at higher oscillation frequencies. At 150 μm/s sliding speed, they observed no friction-reducing effect from oscillations at any frequency; oscillation speeds were below the sliding speed at the coupling frequency and mechanical coupling became inadequate at higher oscillation frequencies.

These results have been primarily interpreted through the Prandtl-Tomlinson framework for atomic scale friction [32–34]. When a probe rests against an opposing surface, it sits in a well of minimal potential energy [35]. The lateral force needed to activate a jump from one well to the next depends on the depth of the well, E_0. When the probe vibrates within the well due to thermal or mechanical energy, the lateral force needed to activate slip decreases; in this way, vibration-activated lubricity is the mechanical analog to thermolubricity [36, 37]. According to this framework, radically reduced friction can be expected when the oscillation amplitude approaches or exceeds the distance between wells and the oscillation speed exceeds the sliding speed [9].

Nonetheless, robust vibration-activated lubricity has proven elusive in practice. This is primarily due to the difficulty in transmitting the external vibrational energy (whose attributes can be measured and controlled) to the contact interface (whose attributes are unknown, uncontrollable, and unpredictable). In each of the experimental studies we reviewed, the friction-reducing effect only occurred at a specific coupling frequency and only if the oscillation speeds exceeded the sliding speed. Given the low resonance frequencies (< 20 kHz) of a typical instrument and the atomic scale slip lengths of these tribo-systems, vibration-activated lubricity has thus far been limited to impractically slow speeds (*e.g.* $V < 20$ kHz·0.2 nm = 4 μm/s) [8, 31, 38]. Furthermore, as Socoliuc *et al*. point out, the need to simultaneously couple the drive to a diversity of interfacial springs within multi-asperity contacts is a significant limitation for macroscale and even microscale applications [38].

The primary aim of this paper was to resolve the current experimental limitations of vibration-activated lubricity. We hypothesize that robust vibration-activated lubricity can be achieved, with little or no

sensitivity to interfacial, tribological, or mechanical details, if oscillations can be applied directly to the sample (*i.e.* without needing mechanical coupling). We test this hypothesis here by coating the quartz crystal microbalance (QCM) with our sample material, which enforced a direct link between the oscillator and the sample, and by measuring friction for varying materials, instruments, and tribological conditions with and without QCM oscillations. By including multi-asperity microscale contacts of varying size, this paper also tests the hypothesis that vibration-activated lubricity becomes more difficult as the number of asperities in contact (interfacial springs) increases [38].

2.0 Methods

This study uses either of two materials for the counter sample: gold, a model noble metal, and single crystal MoS_2, a model lamellar solid. Both sample materials were applied directly to the quartz crystal microbalance (QCM) crystals. These QCM crystals were AT-cut to resonate laterally at 5 MHz (Q-Sense QSX 301) and coated with gold by the manufacturer to an average roughness of 5 nm over a 10 μm measurement window. With our system, direct STM measurements have shown that the QCM oscillates over 1–10 nm, depending on the quality factor. Single crystal MoS_2 surfaces were created through progressive exfoliation. First, a mineralogical single crystal MoS_2 (Structure Probe, Inc.) fragment was adhered on top of the gold-coated QCM crystal using a ~ 0.03 mL drop of polyurethane clear gloss adhesive. Scotch tape was then used to thin the MoS_2 sample through exfoliation until the measured impedance of the QCM dropped to 30Ω (20–25Ω as received). Finished MoS_2 samples were ~ 200 nm thick and 2 nm rough. AFM profilometry revealed that these surfaces were basally oriented and atomically smooth with occasional ~ 0.7 nm high steps reflecting subsurface edge sites [39].

Two friction measurement devices, a custom microtribometer and an AFM, were used to vary the resonant properties of the system. The microtribometer comprised a high resolution nanopositioning stage (PI P-628.1CD) with a range of 800 μm and a resolution of < 2 nm for lateral reciprocation, a vertical nanopositioning stage (PI Q-545.240) with a range of 26 mm and a resolution of 6 nm, and two orthogonal capacitive displacement sensors (Lion Precision CPL290, C3S) for measuring normal and friction forces on cantilevers of varying stiffness (190–1200 N/m normal stiffness, 80–700 N/m lateral stiffness and 200–1000 Hz normal resonant frequencies) [39, 40]. The AFM used in this study is the Dimension 3100V.

Polycrystalline α-Al2O3 spheres (microspheresnanospheres.com) were used as the probe material for their high hardness, chemical inertness, and availability in a range of diameters. These alumina spheres were mounted to the appropriate cantilever prior to friction measurement using a custom micromanipulation setup described in detail previously [41, 42]. The microtribometry experiments used 50, 100, and 1500 μm diameter spheres on custom cantilevers of varying stiffness. The AFM experiments used a 50 μm alumina colloid from the same batch, mounted to a 200 N/m normal stiffness (525 kHz resonant frequency) AFM cantilever (Bruker RTESPA-525); in this case, the sphere was located 42 μm from the fixed end of the cantilever to increase load capacity. The normal and lateral stiffnesses and

force constants were calibrated using the TLFC method [42] (k_{normal} = 3900 ± 200 N/m, $k_{lateral}$ = 1770 ± 70 N/m).

The experiments in this study quantified if, to what extent, and under what range of conditions QCM oscillations at the interface reduced the apparent friction. Friction was measured as a function of load, which was ramped up to a probe size-dependent maximum value (up to 5 mN) and then back down to the minimum value to capture any effects from wear and transfer. Three or four reciprocation cycles were run at each load. Repeat experiments were conducted with the same probe but at independent locations on the substrate. The ordering of the experiments was randomized to eliminate any systematic effects from wear or material transfer. In addition to varying the measurement load, instrument, probe radius, and sample material, we varied the sliding speed from 5 μm/s to 1 mm/s. The nominal speed was fixed at 50 μm/s for all non-variable speed experiments and the reciprocating frequency was fixed at 0.5 Hz (e.g. 50 μm/s on a 50 μm track) for all experiments.

QCM lateral displacements are expected to be in the range of 1–10 nm depending on experimental variables (load, friction, dissipation, etc.) [39, 43]. Given a fixed oscillation frequency of 5 MHz, the average oscillation speed is expected to be between 10 and 100 mm/s, which is at least an order of magnitude faster than the maximum sliding speed of the instrument (1 mm/s). The expected oscillation length is ~ 2-10-fold larger than the relevant lattice constants but > 100-fold smaller than the contact diameter, the asperity length scale, and the reciprocation length as illustrated in Fig. 1.

3.0 Results

Friction results from microtribometry experiments with a 50 μm alumina sphere sliding on gold at 50 μm/s are shown with and without oscillations in Fig. 2 (recall that oscillations occur when alternating current is supplied to the QCM electrodes; otherwise, the QCM acts as a static substrate). Without oscillations, we observed a typical friction response with variable friction across the track, a relatively linear dependence on normal force, and a modest friction coefficient of 0.179 ± 0.003 [39]. QCM oscillations reduced variations across the friction loop and reduced the friction coefficient to 0.012 ± 0.004. To our knowledge, this is the first observation of vibration-activated lubricity using an oscillation frequency (5 MHz) that exceeds the resonant frequency of the instrument (~ 200 Hz) by many orders of magnitude.

Results from repeat experiments using the AFM are shown in Fig. 3. In this case, the probe (50 μm alumina), substrate, and sliding frequency were identical but loads (100–500 μN), track length (25 μN), and sliding speed (25 μm/s) were slightly less. The measured friction coefficients were 0.186 ± 0.004 and 0.035 ± 0.002 with oscillations Off and On, respectively. These results are consistent with those obtained from the microtribometer despite a ~ 10-fold difference in cantilever stiffness and a 1,000-fold difference in instrument resonant frequency. These important instrument-specific variables had no effect on vibration-activated lubricity here, presumably, because the oscillations were applied directly to the gold surface. Interestingly, QCM oscillations had no obvious friction reducing effect when experiments were

repeated with the stock cantilever (8 nm reported Si tip radius = 16 nm diameter). The loads were limited by reduced cantilever stiffness, but the results from the sharp probe with oscillations appear to intersect with the results from an alumina colloid without oscillations.

Results from repeat microtribometry experiments with probes of varying diameter (50-1500 μm) are shown in Fig. 4. At ~ 2 mN of load, friction loops were wide/irregular without QCM oscillations and thin/stable with QCM oscillations (Fig. 4A) despite the large differences in probe diameter, contact diameter, and contact pressure. For all probes and at all loads, the friction force increased with the normal force (Fig. 4B) with average slopes of ~ 0.16–0.18 without QCM oscillations and ~ 0.01–0.02 with QCM oscillations (Fig. 4C). We did, however, observe a transition to high friction for the smallest (50 μm diameter) probe when the loads exceeded 2.5 mN (transition indicated and post-transition data made partially transparent); we discuss a possible cause for this transition in the discussion section.

The original microtribometry experiments (Fig. 2) were repeated for alumina against single crystal MoS_2 and the results are shown in Fig. 5. In the absence of oscillations, friction was smaller in magnitude and more stable across the wear track for MoS_2 substrates than for gold substrates; this is consistent with the known solid lubricity of MoS_2. In the presence of oscillations, friction loops collapsed for alumina against single crystal MoS_2 just as they did against gold under the same conditions. With oscillations, friction coefficients were 0.017 ± 0.007 against single crystal MoS_2 compared to 0.012 ± 0.004 against gold. It is noteworthy that these materials produced similar friction coefficients during oscillation given their very different frictional properties of these materials [44, 45] (0.179 ± 0.003 for gold and 0.04 ± 0.007 for single crystal MoS_2 in the absence of oscillations).

The results of variable sliding speed microtribometry measurements are shown in Fig. 6 for gold against 50 and 100 μm alumina probes. Friction did not depend significantly on speed from 5-1000 μm/s or on probe size. Without oscillations, friction of alumina on gold varied from 0.15 to 0.21. With oscillations, friction varied from 0.01 to 0.04; the presence of oscillations reduced friction by 80–95% for both probes and at all speeds.

Finally, we conducted a sloped-track experiment designed to test whether normal surface separation contributes to the friction reductions. In this experiment, the oscillating QCM was tilted as illustrated in Fig. 7 to ensure that the probe makes and breaks contact during each reciprocation cycle. At location (1) the probe floats above the surface and experiences no normal or frictional forces. At location (2), the probe snaps into contact (Fig. 7B). Load peaks at location (3) and begins to decrease at (4). At location (5) the probe experiences significant net tension from adhesion while maintaining finite friction despite the 5 MHz oscillations. Thus, while it is possible that lateral resonance of the QCM may have a normal component, that normal component was not sufficient to separate surfaces even under moderate tension. Interestingly, we observed significant (non-zero) friction under negative load until the contact fails under maximum tension at location (6).

4.0 Discussions

This study demonstrated robust vibration-activated lubricity; to our knowledge, this is the first such demonstration. Subjecting microscale tribological contacts directly to QCM oscillations reduced friction coefficients to ~ 0.01–0.05 regardless of load, sliding speed, probe size, substrate material, instrument, and cantilever stiffness. This is in contrast to prior observations, which report vibration-activated lubricity as being limited to relatively narrow sets of experimental conditions. Specifically, previous studies show the loss of vibration-activated lubricity when the oscillation frequency deviated more than several-fold from the resonant frequency of the instrument or when the oscillation speed was less than the sliding speed. For example, Riedo *et al*. observed drastically reduced friction but only when the oscillation frequency was comparable to the resonant frequency of the instrument and only at relatively slow sliding speeds (at 8 μm/s but not at 150 μm/s) [8]. Similarly, Jeon *et al*. found that friction increased by at an order of magnitude or more when the oscillation frequency was much less than or greater than the resonant frequency of their system (~ 20 kHz) [30]. We detected no such limitations from instrument resonance or sliding speed. We observed vibration-activated lubricity at sliding speeds between 5 and 1,000 μm/s using a constant 5 MHz oscillation frequency with two instruments whose resonant frequencies were 10 to 10,000-fold smaller (~ 525 kHz and ~ 200 Hz). This is in direct contrast to previous studies, which consistently show the disruption of vibration-activated lubricity at very high oscillation frequency (relative to instrument resonance) [8, 9, 30].

We attribute these unusual findings to two key features of our experiments. The first is that oscillations of prescribed frequency were applied directly to the substrate. In most other studies, the oscillator had to be coupled mechanically to the sample through an intervening spring/mass system. In our case, the substrate oscillated at the prescribed QCM frequency without any requirement for mechanical coupling to the instrument. Additionally, because the oscillation speeds were likely between 10 and 100 mm/s, we were able to maintain vibration-activated lubricity up to 1 mm/s, the maximum sliding speed of either instrument. In effect, this approach decoupled the vibration-activated lubricity phenomenon from the instrument and other experimental variables.

As our sharp probe experiments (Fig. 3A and 3B) demonstrate, direct oscillation of the substrate doesn't guarantee robust vibration-activated lubricity. Jeon *et al.* made similar observations during direct oscillation experiments with sharp AFM probes [30]. Like us, they found no friction reducing effect from substrate oscillations when the oscillation frequency was much larger than the resonant frequency of the cantilever. This observation, that robust vibration-activated lubricity breaks down below some critical length scale conflicts with the hypothesis that it is more difficult to achieve in multi-asperity contacts compared to single-asperity contacts [38].

The key difference, we propose, is the relative ease with which nanoscale and microscale probes can track the oscillating substrate. Consider our sharp AFM probe, which had a radius of ~ 8 nm and an estimated contact stiffness of ~ 100 N/m. Assuming 5 MHz oscillations on a 2 mm long track, the inertial force (tip mass times peak acceleration ~ 1 fN) and spring force (100 nN) were below the friction force (~ 1μN = 0.2·5 μN). Thus, we expect friction to have prevented the interfacial slip necessary to cause vibration-activated lubricity. Jeon *et al*. [30] restored vibration-activated lubricity by oscillating the

substrate near cantilever resonance; this, we propose, activates large tip displacements that break the frictional contact. This would help explain why nanoscale examples of vibration-activated lubricity have, thus far, been limited to oscillation frequencies in the vicinity of resonance [8, 9, 30].

By contrast, consider the 50 μm diameter probe. In this case, the inertial force of the oscillating probe alone would be ~ 500 μN (negligible spring force). Assuming a 0.2 friction coefficient, we would expect the probe to slip at normal loads below 2.5 mN and stick to the oscillating substrate at greater loads; remarkably (and likely coincidentally), this anticipated transition is equal to the observed transition (Fig. 4B). Increasing the probe diameter to 100 μm increases the expected critical load to 18 mN, well beyond our maximum load of 5 mN. The critical load for the 1.5 mm diameter probe is expected to approach 6 N. Multi-asperity contacts may impede vibration-activated lubricity when mechanical coupling is needed; this study shows that multi-asperity contacts promote vibration-activated lubricity when the need for mechanical coupling is eliminated.

By eliminating the dependence on mechanical coupling, we were also able to overcome the limitations on sliding speed previously observed. In the study by Riedo *et al.* [8], vibration-activated lubricity vanished when they increased sliding speeds from 8 μm/s to 150 μm/s. In that case, the maximum speed was limited by the oscillation speed, which was limited by the resonance characteristics of the instrument. Here, we had no such limitations from instrument resonant frequency, which was as low as 200 Hz. In this case, we were limited by the maximum sliding speed of the instrument, but beyond that we were only limited by the speed of the oscillator, which was likely between 10 and 100 mm/s.

Finally, our results provide direct experimental evidence that normal ‘hopping’ was not a significant contributor to the friction-reducing effect of oscillation. The best evidence prior to this study was interferometry data showing minimal interfacial dilatation during oscillation [23]. We were able to maintain interfacial tension and a small but positive friction force during QCM oscillation. Thus, while it is clear that hopping does have a significant friction reducing effect, it is also true that purely lateral oscillations can provide similar effects without any need for changes in normal force. Thus, vibration-activated lubricity can occur due to normal hopping or due to purely lateral oscillations that reduce or overcome the barriers to slip.

1. **Closing Remarks**

5.0 Closing Remarks

1. Contrary to prior studies showing that vibration-activated lubricity is limited to a very specific set of conditions, this study demonstrated sustained vibration-activated lubricity for a wide range of materials, instrument attributes, and tribological conditions. To our knowledge, this is the first demonstration of ‘robust’ vibration-activated lubricity.

2. In the presence of direct QCM oscillations at 5 MHz, friction coefficients in microscale multi-asperity contacts were consistently between 0.01-0.05 irrespective of the probe size (50-1500 μm), instrument

(Microtribometer and AFM), material system (alumina on gold or MoS_2), sliding speed (5-1000 μm/s), cantilever resonance frequency (0.2-525 KHz) and cantilever stiffness (k_n= 190-3900 N/m). In the absence of oscillations, friction coefficients were between 0.15-0.21 for alumina on gold and 0.03-0.05 for alumina on MoS_2.

3. Friction reduction did not involve contact separation or 'hopping' as demonstrated by our ability to sustain measurable tension during sliding in the presence of oscillations. Thus, we can attribute the effect to relative slip in the lateral direction alone.

4. Our findings suggest that the following satisfy the conditions for robust vibration-activated lubricity: (1) direct coupling between the oscillator and the substrate; (2) probe inertial or spring forces >> available interfacial friction; (3) oscillation speed >> sliding speed; (4) oscillation amplitude ≅ or > the slip length.

6.0 Declarations

Funding: The authors gratefully acknowledge financial support from the NSF 1434435 for financial support of this work.

Conflict of interest: The authors have no conflicts of interest to declare that are relevant to the content of this article.

Availability of data and material: Not applicable

Code availability: Not applicable

7.0 References

1. Guerra, R., Vanossi, A., Urbakh, M.: Controlling microscopic friction through mechanical oscillations. Phys. Rev. E - Stat. Nonlinear, Soft Matter Phys. **78**, 1–5 (2008). doi:10.1103/PhysRevE.78.036110
2. Roth, R., Fajardo, O.Y., Mazo, J.J., Meyer, E., Gnecco, E.: Lateral vibration effects in atomic-scale friction. Appl. Phys. Lett. **104**, 083103 (2014). doi:10.1063/1.4866427
3. Capozza, R., Vanossi, A., Vezzani, A., Zapperi, S.: Suppression of Friction by Mechanical Vibrations. Phys. Rev. Lett. **103**, 085502 (2009). doi:10.1103/PhysRevLett.103.085502
4. Teidelt, E., Starcevic, J., Popov, V.L.: Influence of Ultrasonic Oscillation on Static and Sliding Friction. Tribol. Lett. **48**, 51–62 (2012). doi:10.1007/s11249-012-9937-4
5. Wang, P., Ni, H., Wang, R., Li, Z., Wang, Y.: Experimental investigation of the effect of in-plane vibrations on friction for different materials. Tribol. Int. **99**, 237–247 (2016). doi:10.1016/j.triboint.2016.03.021
6. Gutowski, P., Leus, M.: The effect of longitudinal tangential vibrations on friction and driving forces in sliding motion. Tribol. Int. **55**, 108–118 (2012). doi:10.1016/j.triboint.2012.05.023

7. Lantz, M.A., Wiesmann, D., Gotsmann, B.: Dynamic superlubricity and the elimination of wear on the nanoscale. Nat. Nanotechnol. **4**, 586–591 (2009). doi:10.1038/nnano.2009.199
8. Riedo, E., Gnecco, E., Bennewitz, R., Meyer, E., Brune, H.: Interaction Potential and Hopping Dynamics Governing Sliding Friction. Phys. Rev. Lett. **91**, 1–4 (2003). doi:10.1103/PhysRevLett.91.084502
9. Popov, V.L., Starcevic, J., Filippov, A.E.: Influence of ultrasonic in-plane oscillations on static and sliding friction and intrinsic length scale of dry friction processes. Tribol. Lett. **39**, 25–30 (2010). doi:10.1007/s11249-009-9531-6
10. Dinelli, F., Biswas, S.K., Briggs, G.A.D., Kolosov, O.V.: Ultrasound induced lubricity in microscopic contact. Appl. Phys. Lett. **71**, 1177–1179 (1997). doi:10.1063/1.120417
11. Klafter, J., Urbakh, M.: The Basic of Nanoscale Friction and Ways to Control it. Presented at the: (2007)
12. Capozza, R., Vanossi, A., Vezzani, A., Zapperi, S.: Triggering Frictional Slip by Mechanical Vibrations. Tribol. Lett. **48**, 95–102 (2012). doi:10.1007/s11249-012-0002-0
13. Wang, P., Ni, H., Wang, R., Liu, W., Lu, S.: Research on the Mechanism of In-Plane Vibration on Friction Reduction. Materials (Basel). **10**, 1015 (2017). doi:10.3390/ma10091015
14. Pedraz, P., Wannemacher, R., Gnecco, E.: Controlled Suppression of Wear on the Nanoscale by Ultrasonic Vibrations. ACS Nano. **9**, 8859–8868 (2015). doi:10.1021/acsnano.5b02466
15. Bureau, L., Baumberger, T., Caroli, C.: Shear response of a frictional interface to a normal load modulation. Phys. Rev. E - Stat. Physics, Plasmas, Fluids. Relat. Interdiscip. Top. **62**, 6810–6820 (2000). doi:10.1103/PhysRevE.62.6810
16. Giacco, F., Lippiello, E., Ciamarra, M.P.: Solid-on-solid single-block dynamics under mechanical vibration. Phys. Rev. E. **86**, 016110 (2012). doi:10.1103/PhysRevE.86.016110
17. Hölscher, H., Schirmeisen, A., Schwarz, U.D.: Principles of atomic friction: from sticking atoms to superlubric sliding. Philos. Trans. R. Soc. A Math. Phys. Eng. Sci. **366**, 1383–1404 (2008). doi:10.1098/rsta.2007.2164
18. Park, J.Y., Salmeron, M.: Fundamental Aspects of Energy Dissipation in Friction. Chem. Rev. **114**, 677–711 (2014). doi:10.1021/cr200431y
19. Socoliuc, A., Gnecco, E., Maier, S., Pfeiffer, O., Baratoff, A., Bennewitz, R., Meyer, E.: Atomic-scale control of friction by actuation of nanometer-sized contacts. Science (80-.). **313**, 207–210 (2006). doi:10.1126/science.1125874
20. Skåre, T., Ståhl, J.-E.: Static and dynamic friction processes under the influence of external vibrations. Wear. **154**, 177–192 (1992). doi:10.1016/0043-1648(92)90253-5
21. Van X. Nguyen, Golikov, N.S.: Analysis of material particle motion and optimizing parameters of vibration of two-mass GZS vibratory feeder. J. Phys. Conf. Ser. **1015**, 052020 (2018). doi:10.1088/1742-6596/1015/5/052020
22. Boer, D., Mayer, T.M.: T ribology of MEMS. Society. **26**, 302–304 (2001)

23. Heuberger, M., Drummond, C., Israelachvili, J.: Coupling of normal and transverse motions during frictional sliding. J. Phys. Chem. B. **102**, 5038–5041 (1998). doi:10.1021/jp9823143
24. Bhushan, B.: Nanotribology and nanomechanics of MEMS/NEMS and BioMEMS/BioNEMS materials and devices. Microelectron. Eng. **84**, 387–412 (2007). doi:10.1016/j.mee.2006.10.059
25. Zhu, H.W., Shi, Q.F., Li, L.S., Yang, M., Xu, A., Zheng, N.: Frictional effect of bottom wall on granular flow through an aperture on a conveyor belt. Powder Technol. **367**, 421–426 (2020). doi:10.1016/j.powtec.2020.03.067
26. Jiang, C., Huang, J., Jiang, Z., Qian, D., Hong, X.: Estimation of Energy Savings When Adopting Ultrasonic Vibration-Assisted Magnetic Compound Fluid Polishing. Int. J. Precis. Eng. Manuf. - Green Technol. **8**, 1–11 (2021). doi:10.1007/s40684-019-00167-5
27. Polycarpou, A.A., Soom, A.A.: Closure to "Discussion of 'Boundary and Mixed Friction in the Presence of Dynamic Normal Loads: Part II—Friction Transients'": (1995, ASME J. Tribol., 117, p. 748). J. Tribol. (1995). doi:10.1115/1.2831549
28. Van Spengen, W.M., Wijts, G.H.C.J., Turq, V., Frenken, J.W.M.: Microscale friction reduction by normal force modulation in MEMS. J. Adhes. Sci. Technol. **24**, 2669–2680 (2010). doi:10.1163/016942410X508226
29. Capozza, R., Vanossi, A., Vezzani, A., Zapperi, S.: Suppression of friction by mechanical vibrations. Phys. Rev. Lett. **103**, 1–4 (2009). doi:10.1103/PhysRevLett.103.085502
30. Jeon, S., Thundat, T., Braiman, Y.: Effect of normal vibration on friction in the atomic force microscopy experiment. Appl. Phys. Lett. **88**, 1–4 (2006). doi:10.1063/1.2203741
31. Socoliuc, A.: Atomic-Scale Control of Friction by Actuation of Nanometer-Sized Contacts. Science (80-.). **313**, 207–210 (2006). doi:10.1126/science.1125874
32. Popov, V.L., Gray, J.A.T.: Prandtl-Tomlinson Model: A Simple Model Which Made History. 153–168 (2014). doi:10.1007/978-3-642-39905-3_10
33. Fajardo, O.Y., Gnecco, E., Mazo, J.J.: Out-of-plane and in-plane actuation effects on atomic-scale friction. Phys. Rev. B - Condens. Matter Mater. Phys. **89**, 1–7 (2014). doi:10.1103/PhysRevB.89.075423
34. Müser, M.H.: Velocity dependence of kinetic friction in the Prandtl-Tomlinson model. Phys. Rev. B - Condens. Matter Mater. Phys. 84, (2011). doi:10.1103/PhysRevB.84.125419
35. Carpick, R.W.: Controlling friction. Science (80-.). 313, 184–185 (2006). doi:10.1126/science.1130420
36. Krylov, S.Y., Jinesh, K.B., Valk, H., Dienwiebel, M., Frenken, J.W.M.: Thermally induced suppression of friction at the atomic scale. Phys. Rev. E - Stat. Nonlinear, Soft Matter Phys. **71**, 1–4 (2005). doi:10.1103/PhysRevE.71.065101
37. Jinesh, K.B., Krylov, S.Y., Valk, H., Dienwiebel, M., Frenken, J.W.M.: Thermolubricity in atomic-scale friction. Phys. Rev. B - Condens. Matter Mater. Phys. **78**, 1–12 (2008). doi:10.1103/PhysRevB.78.155440

38. Socoliuc, A., Bennewitz, R., Gnecco, E., Meyer, E.: Transition from stick-slip to continuous sliding in atomic friction: Entering a new regime of ultralow friction. Phys. Rev. Lett. **92**, 1–4 (2004). doi:10.1103/PhysRevLett.92.134301
39. Borovsky, B.P., Garabedian, N.T., McAndrews, G.R., Wieser, R.J., Burris, D.L.: Integrated QCM-Microtribometry: Friction of Single-Crystal MoS2 and Gold from μm/s to m/s. ACS Appl. Mater. Interfaces. **11**, 40961–40969 (2019). doi:10.1021/acsami.9b15764
40. Garabedian, N.T., Bhattacharjee, A., Webster, M.N., Hunter, G.L., Jacobs, P.W., Konicek, A.R., Burris, D.L.: Quantifying, Locating, and Following Asperity-Scale Wear Processes Within Multiasperity Contacts. Tribol. Lett. 67, (2019). doi:10.1007/s11249-019-1203-6
41. Garabedian, N.T., Khare, H.S., Carpick, R.W., Burris, D.L.: AFM at the Macroscale: Methods to Fabricate and Calibrate Probes for Millinewton Force Measurements. Tribol. Lett. **67**, 1–10 (2019). doi:10.1007/s11249-019-1134-2
42. Bhattacharjee, A., Garabedian, N.T., Evans, C.L., Burris, D.L.: Traceable Lateral Force Calibration (TLFC) for Atomic Force Microscopy. Tribol. Lett. **68**, 1–12 (2020). doi:10.1007/s11249-020-01349-y
43. Borovsky, B.P., Bouxsein, C., O'Neill, C., Sletten, L.R.: An Integrated Force Probe and Quartz Crystal Microbalance for High-Speed Microtribology. Tribol. Lett. 65, (2017). doi:10.1007/s11249-017-0933-6
44. Borovsky, B.P., Garabedian, N.T., McAndrews, G.R., Wieser, R.J., Burris, D.L.: Integrated QCM-Microtribometry: Friction of Single-Crystal MoS2 and Gold from μm/s to m/s. ACS Appl. Mater. Interfaces. **11**, 40961–40969 (2019). doi:10.1021/acsami.9b15764
45. Khare, H.S., Burris, D.L.: The extended wedge method: Atomic force microscope friction calibration for improved tolerance to instrument misalignments, tip offset, and blunt probes. Rev. Sci. Instrum. 84, (2013). doi:10.1063/1.4804163

Figures

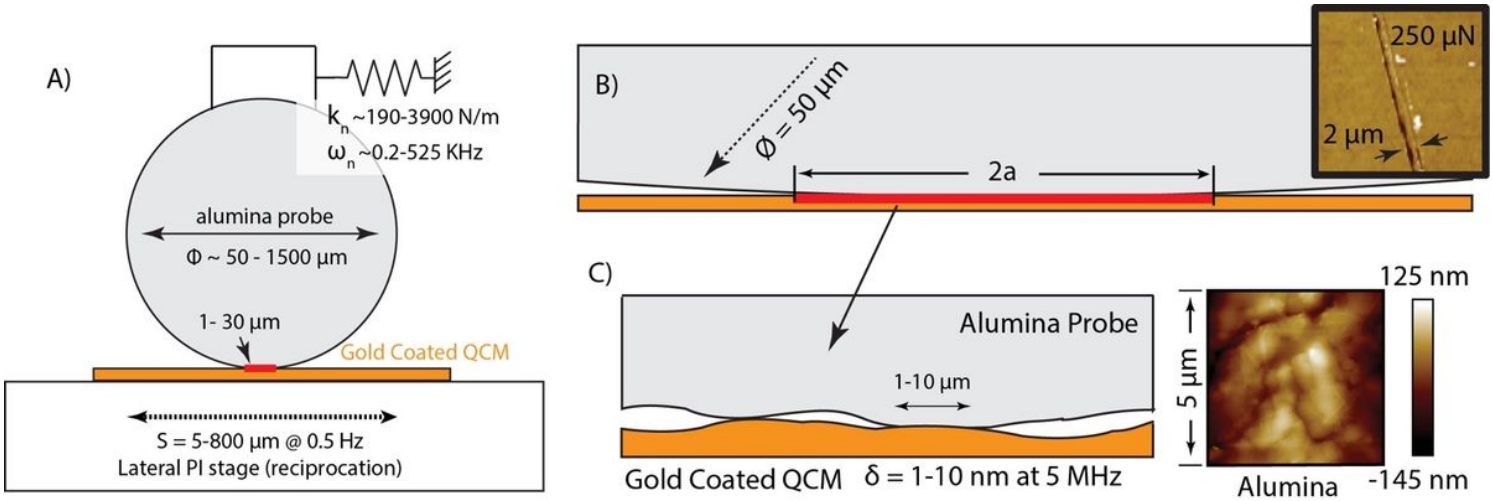

Figure 1

Illustration of the experimental details at varying length scales. (A) The alumina colloid (Φ ~ 50-1500 μm) in contact with the gold-coated QCM. In all experiments, the QCM oscillation frequency (5 MHz) and speed (~100 mm/s) >> cantilever resonance frequency (0.2-525 kHz) and sliding speed (0.005-1 mm/s). (B) The reciprocation length (5-800 μm) > the contact diameter (ca. 1-30 μm) > QCM oscillation length (ca. 1-10 nm). The wear track image of the gold surface was collected via AFM after sliding at 0.25 mN of normal force. (C) The alumina probes are rough with individual asperities of similar dimensions as the contact diameter (left), evidenced by the tapping mode topography scan (right).

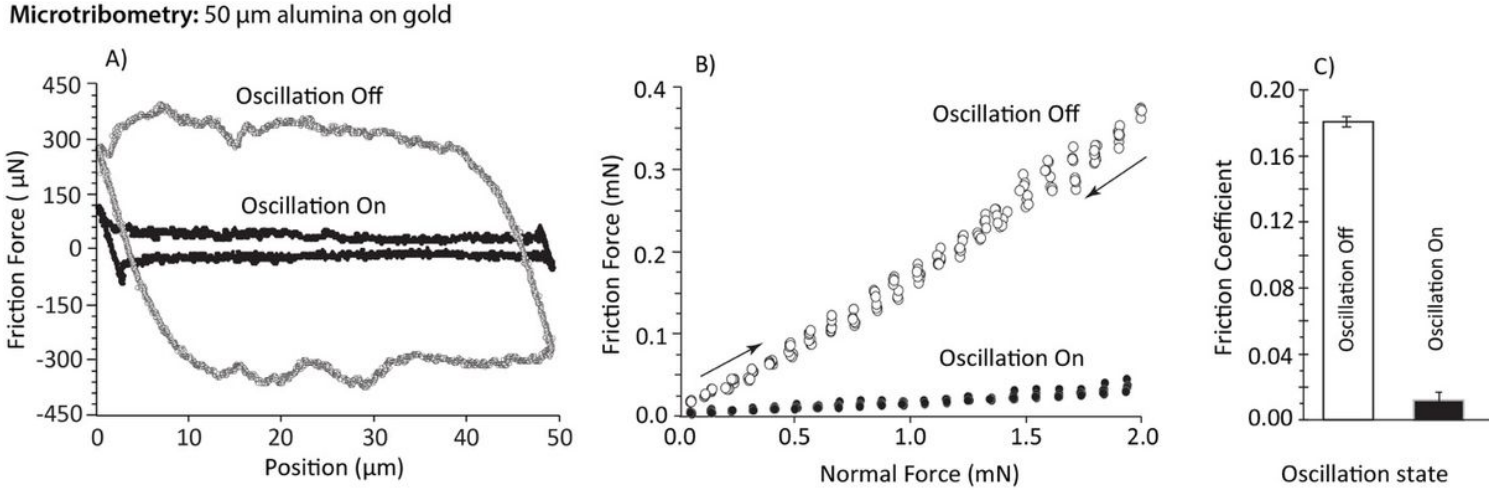

Figure 2

Friction results from a 50 μm diameter alumina colloid against a gold-coated QCM in the microtribometer. External oscillations were Off (open) or On (closed) as noted. (A) Representative friction loops (~2 mN normal force). B) Friction force versus normal force (from 0.05-2 mN) for a representative pair. Load was ramped up and then down to capture effects from wear and transfer. C) Mean and standard deviation for the friction coefficient (slope of friction versus normal force in B) based on n = 3 repeats with oscillations On and Off.

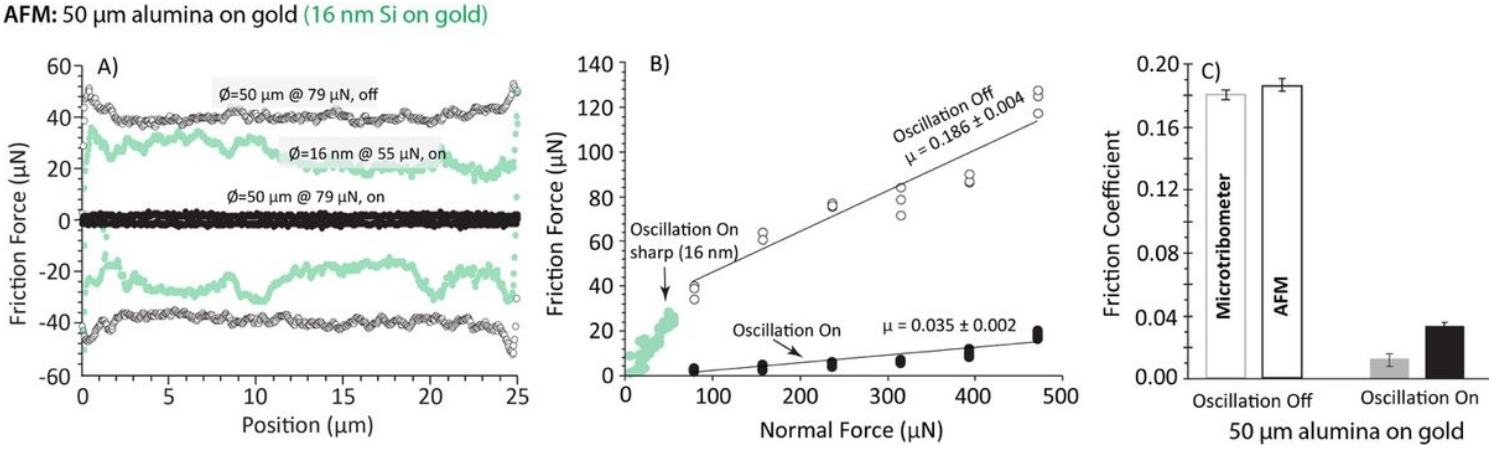

Figure 3

Friction results for AFM experiments. (A) Representative friction loops for 50 μm alumina on gold at 79 μN load with (closed) and without (open) oscillations. The effect from oscillations on the friction of a

sharp probe (unmodified cantilever, 16 nm Si on gold at 55 μN) is shown for reference. B) Friction force versus normal force for the 50 μm alumina probe with and without oscillations. The results of experiments with oscillation on the unmodified cantilever are shown in green. Oscillations only appear to significantly reduce friction when applied with the larger probe. C) Average friction coefficients for 50 μm alumina on gold with and without oscillations in AFM and microtribometer experiments. Error bars represent the standard deviation of n = 2 repeats for AFM measurements and n = 3 repeats for microtribometry measurements.

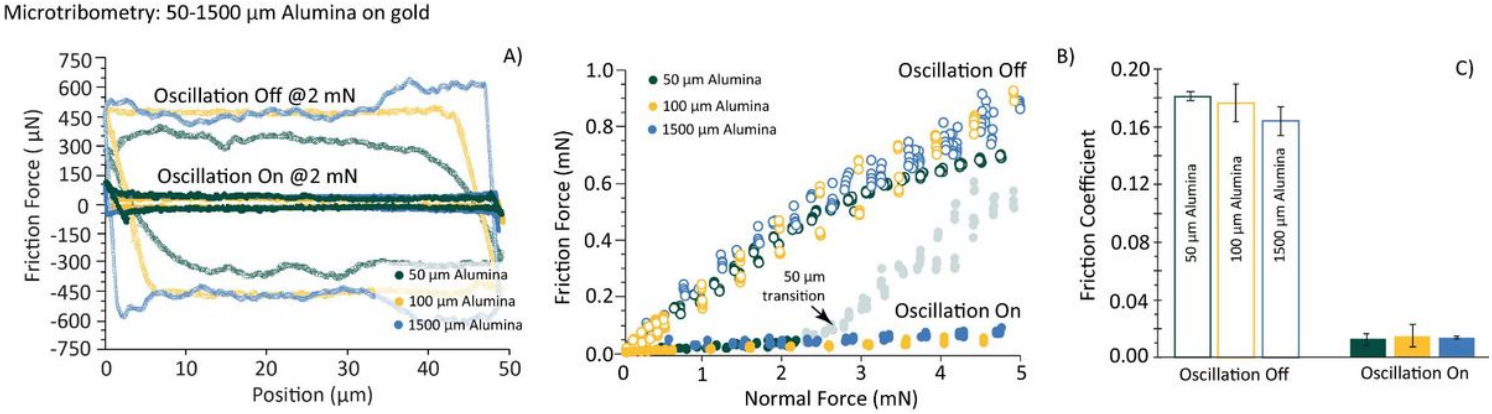

Figure 4

Friction results with alumina probes of three diameters (50 μm, 100 μm and 1500 μm) against a gold-coated QCM with oscillation Off and On. (A) Representative friction loops from alumina on gold at a normal force of ~2 mN. B) Friction force versus normal force for the three probes with and without oscillations. In the case of the 50 μm probe, we observed a transition to high friction beyond 2.5 mN of normal force (shaded). C) Average friction coefficients from three different alumina probes (50-1500 μm) sliding on gold (post-transition data were excluded). Mean and standard deviations are based on n = 3 repeats for 50 μm alumina and n = 2 repeats for 100 and 1500 μm probes with oscillations On and Off.

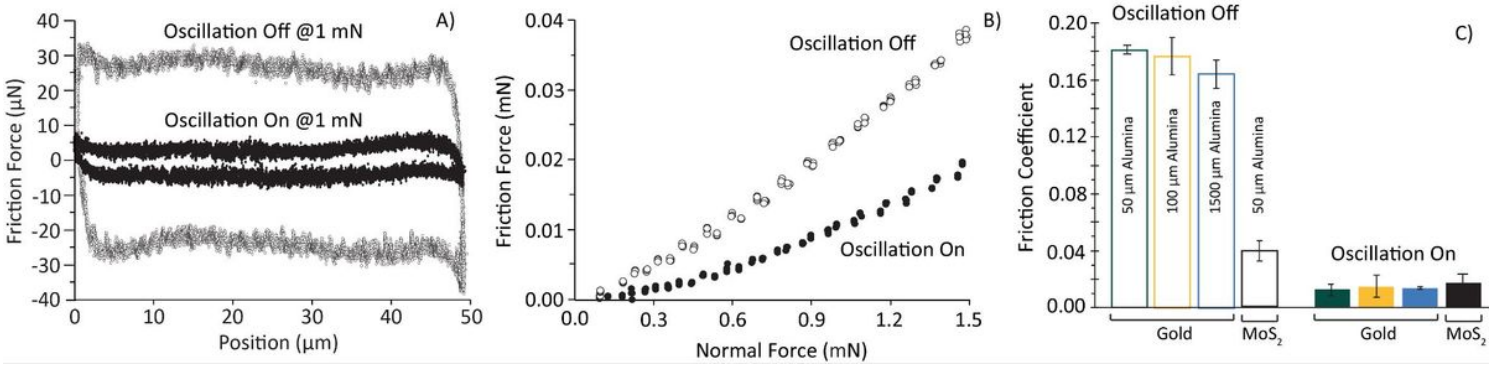

Figure 5

Friction results from microtribometry with a 50 μm diameter alumina colloid against single crystal MoS2 on a QCM with and without oscillation. (A) Representative friction loops from the alumina-MoS2 pair with a normal force of ~1 mN. B) Friction force versus normal force (0.05-1.5 mN) with and without

oscillations. C) Comparative friction coefficient results (50-1500 µm diameter alumina probes on gold and 50 µm diameter alumina on MoS2 adhered QCM. Error bars represent the standard deviation of n = 4 repeats for MoS2 measurements.

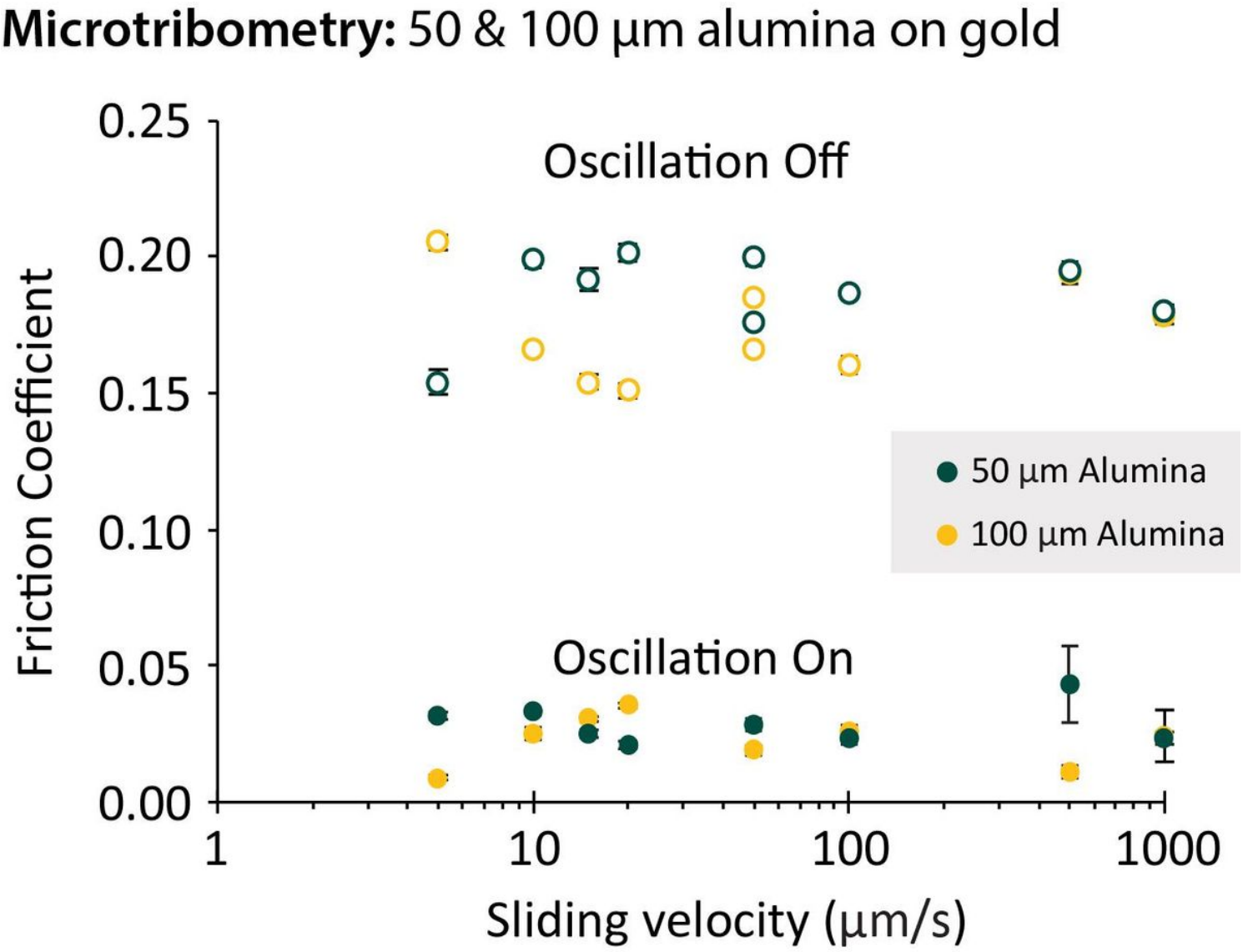

Figure 6

Results of friction experiments conducted with alumina on gold (two probes) at varying sliding speeds (5-1000 µm/s). Green labels represent the 50 µm probe and yellow labels represent the 100 µm probe. Track lengths were varied to maintain a constant sliding frequency to 0.5 Hz. Each experiment was conducted with varied normal force from 0.5 to 1 mN for n = 1 measurement in each case. In this case, the error bars represent the standard error in the linear fit to friction force versus normal force.

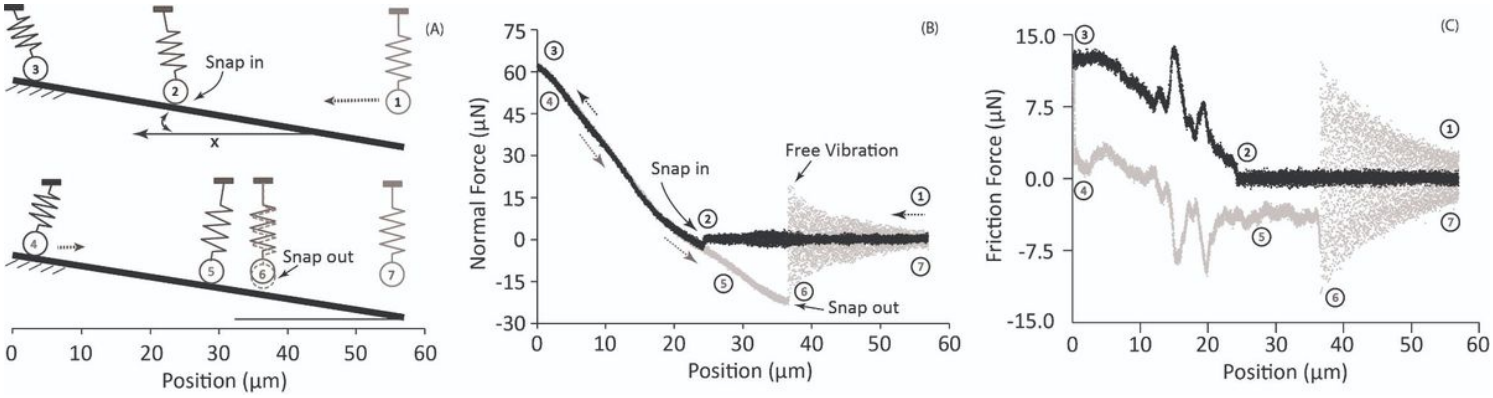

Figure 7

(A) Schematic of a probe sliding in a tilted surface. Probe travels from right (1) to left (3) first and then left (4) to right (7) to complete a sliding cycle. B) Experimental data showing the sliding of the probe in a tilted surface. Black represents the trace/forward part and grey represents the retrace/reverse part of the sliding cycle. ‘Snap in’ occurs at location (2) and ‘snap out’ occurs at location (6).